Wave-current interaction with floating bodies: Experiments and computations

Azin Lamei[a], Shuijin Li[a], Masoud Hayatdavoodi[a,b], H. Ronald Riggs[c] and R. C. Ertekin[b,d]

a. School of Science and Engineering, University of Dundee, Dundee DD1 4HN, UK
b. College of Shipbuilding Engineering, Harbin Engineering University, Harbin, China
c. Civil and Environmental Engineering Dep., University of Hawaii, Honolulu, Hawaii 96822, USA
d. Ocean and Resources Engineering Dep., University of Hawaii, Honolulu, Hawaii 96822, USA

Email: alamei@dundee.ac.uk

Wave-current interaction with floating cylinders is studied by conducting laboratory experiments and by use of the linear diffraction theory with a Green function for small forward speeds. Two cylinders with square and circular water plane areas are considered and their responses to combined waves and current are obtained while freely floating and moored with catenary mooring lines. Motions of the floating cylinders are obtained for codirectional waves and current, and several wave heights and wave periods. Results of the linear theory are compared with the laboratory experiments and discussion is provided.

Introduction

Study of motions of a floating structure to combined waves and current is essential in design and performance analysis of oil and gas platforms, ships and submarines and offshore renewable energy converters, among others. This study focuses on motions of two floating cylinders with square and circular cross sections in the presence of waves and current. The motions of the floating cylinders to combined waves and current is obtained by conducting laboratory experiments and by use of the boundary element method. Boundary element method provides an approximate solution of the wave-current interaction with floating structures, assuming that the current speed (or the forward speed of the structure) is small, *i.e.* $\tau = \dfrac{|U|\,\omega_e}{g} \leq 0.25$, where U is the current speed, ω_e is the encounter frequency and g is the gravitational acceleration, see Zhao & Faltinsen (1988), Taylor (1990) and Noblesse et al. (1995). In this study, a nonsecular expression of the Green function is applied that is defined as a sum of the Green function for zero forward speed and terms due to the forward speed.

In this study, firstly, description of the laboratory experiments and geometry of the floating cylinders are provided. Next, the theory and the applied numerical solution on wave-current interaction with a floating object are presented. Finally, time series of the motions of the two cylinders to combined waves and current for several wave periods and wave heights are presented when *(i)* they are freely floating and *(ii)* moored to the seabed.

Laboratory experiments

The laboratory experiments on wave-current interaction with circular and square cylinders are conducted at the wave-current flume of the University of Dundee. The wave flume is 12 m long and 0.6 m wide and the water depth is fixed at h= 0.3 m in these experiments. Waves are generated by a piston wavemaker and absorbed at the end of the tank by a passive wave absorber. The current is generated by a pump with a fixed flow rate of 40 m^3/h so that the current speed is fixed at 0.06 m/s in this study. The current is uniform across the water depth and codirectional with the incoming waves.

The floating cylinder is placed at the middle of the flume and its motions are recorded by a motion tracking system made by Qualisys. The motion tracking system consists of four motion capture cameras, Arqus A5 with capturing frequency of 100 frames per second, and a video recording camera, Miqus. Each motion capture camera is located at approximately 1 m away from the object. Three wave gauges with 32 Hz sampling frequency are used in the experiments. The free surface elevation upstream and downstream of the object are measured with one and two wave gauges, respectively. The upstream wave gauge (WG1)

is located 1 m upstream from the cylinder and the second and third wave gauges (WG2 and WG3) are located at 1 m and 3 m downstream the of cylinder, respectively. Schematic of the wave-current tank and the arrangements of the mooring lines and the motion tracking system are shown in Figs. 1 (a) and (b), respectively.

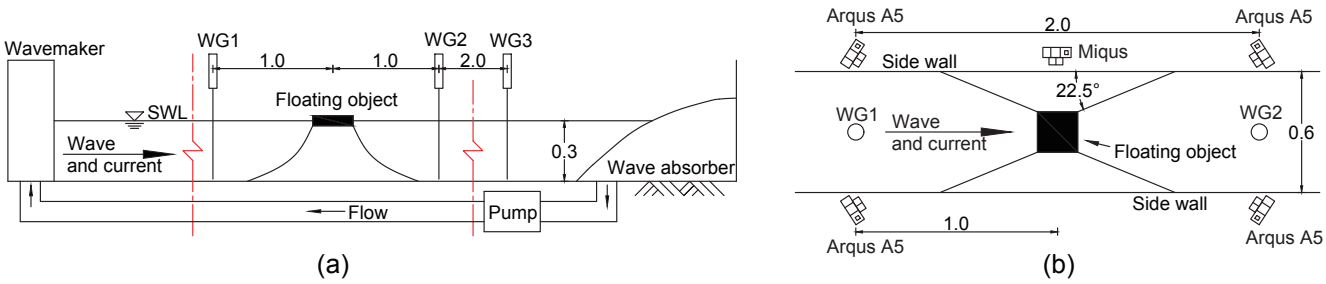

Figure 1: Schematic of (a) the side view and (b) the top view of the wave-current flume used in the laboratory experiments, showing the mooring line arrangements and the motion tracking system. Dimensions are in meter.

Motions of the cylinders with circular and square cross sections due to the combined waves and current are measured in laboratory experiments. The diameter of the circular cylinder and the edges of the square cylinder are 0.2 m, shown in Fig. 2 (The thickness of both cylinders is 50 mm and they are submerged at d = 18 mm). In this study, motions of both freely floating and moored cylinders are considered. Both cylinders are connected to the seabed with four catenary mooring lines, stainless steel chains of long links, with 0.325 m length, 1.5 mm nominal diameter and 193000 MPa modulus of elasticity. The catenary mooring lines are attached to the bottom of the circular cylinder with 22.5° angle with respect to the x- or y-axis. The attachment points of the square cylinder are its four corners at its bottom surface. Combinations of four wave periods (T=1.25 s, 1.5 s, 1.75 s, 2.0 s) with the same wave heights (H=0.3 m) and five wave heights (H=0.2 m, 0.25 m, 0.3 m, 0.35 m, 0.4 m) with the same wave period (T=1.5 s) are considered in the experiments.

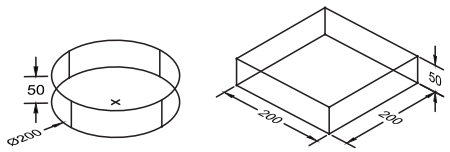

Figure 2: Dimensions (in mm) of the circular and square cylinders considered in this study.

Theory and numerical solution

A moving Cartesian coordinate system is chosen with its origin on the still water level (SWL) that is in steady translation with the mean forward speed of the current. The x-axis is in the same direction as the current speed and its z-axis points upwards. Assuming the flow is irrotational and that the forward speed and the wave amplitude are small and the viscous forces are negligible, the hydrodynamic loads on the structure are obtained with linear diffraction wave theory. The steady flow due to the current is described with a double body flow. Thus, the total velocity potential, $\psi\,(x, y, z, t)$, equals the sum of steady velocity potential, $\bar{\phi}_s\,(x, y, z)$ and time harmonic velocity potentials, $\Phi(x, y, z, t) = \phi(x, y, z)\, e^{i\,\omega_e\,t}$,

$$\psi\,(x, y, z, t) = |U|\,(\bar{\phi}_s\; -\; x) + \Re\{\phi\, e^{i\,\omega_e\,t}\}. \tag{1}$$

where $\omega_e = \omega - |U|\,k\cos\beta$ is the encounter frequency, and ω and β are the incoming wave frequency and the incoming wave heading angle, respectively. The steady velocity potential satisfies the below boundary conditions on the free surface, S_F and the body surface S_B,

$$\frac{\partial \bar{\phi}_s}{\partial z} = 0, \quad \text{on } S_F, \qquad \frac{\partial \bar{\phi}_s}{\partial n} = n_x, \quad \text{on } S_B, \tag{2}$$

where n is the normal vector on the body surface, $n = (n_x, n_y, n_z)$, pointing out of the fluid. The harmonic velocity potential is given as, $\phi = \phi^I + \phi^L + \tau\phi^N$, with ϕ^I the incoming wave velocity potential,

and ϕ^L and ϕ^N representing the linear and nonlinear velocity potentials in both diffraction and radiation problems. The nonlinear velocity potential is a term due to the interaction of wave radiation-diffraction with the local steady flow at the free surface. By implementing the radiation and diffraction boundary conditions on S_F and S_B, the linear and nonlinear velocity potentials, ϕ^L and ϕ^N are computed. ϕ^L and ϕ^N satisfy the below boundary conditions in both diffraction and radiation problems on the free surface,

$$-\frac{\omega_e^2}{g}\phi^L + 2i\tau\frac{\partial\phi^L}{\partial x} + \frac{\partial\phi^L}{\partial z} = 0, \quad \text{on } S_F, \qquad -\frac{\omega_e^2}{g}\phi^N + 2i\tau\frac{\partial\phi^N}{\partial x} + \frac{\partial\phi^N}{\partial z} = Q, \quad \text{on } S_F, \tag{3}$$

where Q is computed as,

$$Q = 2\,i\,\nabla\bar{\phi}_s\,\nabla(\phi^I + \phi^L) - i\,(\phi^I + \phi^L)\,\frac{\partial^2\bar{\phi}_s}{\partial z^2}, \quad \text{on } S_F. \tag{4}$$

Furthermore, the boundary conditions on the wetted surface of the body for the linear and nonlinear velocity potentials are given as,

$$\frac{\partial\phi^L}{\partial n} = -\frac{\partial\phi^I}{\partial n}, \qquad \frac{\partial\phi^N}{\partial n} = 0, \quad \text{on } S_B, \text{ diffraction problem}, \tag{5}$$

$$\frac{\partial\phi^L}{\partial n} = n_j, \qquad \frac{\partial\phi^N}{\partial n} = \frac{i\,m_j}{k}, \quad \text{on } S_B, \text{ radiation problem}, \tag{6}$$

where m_j terms are defined by the double derivatives of the steady velocity potential on the body surface, see Chen & Malenica (1998) for more details.

The harmonic velocity potentials are obtained with boundary integral equations, using the nonsecular Green function for small forward speed, $\tau \leq 0.25$, see Noblesse et al. (1995) and Chen & Malenica (1998). Once the steady, linear and nonlinear velocity potentials are determined, the pressure is obtained by Euler's integrals, Eq. (7) and then the first order excitation forces and moments and added mass and damping coefficients are calculated by integrating the pressure,

$$p = -\rho\Big(g\,z - i\,\omega_e\,(\phi^I + \phi^L + \tau\phi^N) + U\,\nabla\,(\bar{\phi}_s - x)\,\nabla(\phi^I + \phi^L)\Big). \tag{7}$$

Finally, assuming $\tau \leq 0.25$, the equation of motions of a floating body due to combined waves and current is formulated as,

$$\xi_k\,\Big(-\omega_e^2\,(M_{jk} + a_{jk}) + i\,\omega_e b_{jk} + c_{jk,\text{hst}} + c_{jk,\text{moor}}\Big) = A\,F_j^{exc}, \quad j,k = 1,2,\cdots,6, \tag{8}$$

where A is the wave amplitude and $c_{jk,\text{hst}}$ and $c_{jk,\text{moor}}$ are the hydrostatic and mooring lines stiffness coefficients, receptively. ξ_k is the complex body response phasor in mode k and M_{jk} is the linearised body inertia mass matrix. The response amplitude operators (RAOs) of the structure to waves and current for $\tau \leq 0.25$, $|\frac{\xi_k}{A}|$, are obtained by solving Eq. (8) at encounter frequency ω_e.

The numerical solution of the wave-current interaction with the floating cylinders is obtained in HYDRAN-XR, see NumSoft Technologies (2020), modified for this study.

Results and Discussion

Wave-current interaction with floating cylinders with square and circular water plane areas are discussed in this section. Time series of the motions of the floating cylinders in surge, heave and pitch are computed and compared with laboratory experiments when they are freely floating and moored to the seabed, see Fig. 3.

The computed surge and heave motions of the freely floating cylinders are in good agreement with the laboratory measurements for incoming wave period T = 1.25 s whereas at T = 1.5 s, the numerical surge and heave time series of both freely floating cylinders are overestimated compared with the laboratory measurements. Furthermore, in the absence of the mooring lines, the pitch motions of the cylinders in

the laboratory experiments are nonlinear. Nonetheless, the numerical results show a good agreement with measured pitch motions of the cylinders, see Fig. 3(a).

Shown in Fig. 3(b), the surge, heave and pitch motions of the moored cylinders are compared with the laboratory measurements. The numerical surge motions of the circular and square cylinders are slightly smaller and larger, respectively, compared with their counterparts of the laboratory measurements at both incoming wave periods. The heave motions of both cylinders are approximately comparable at T = 1.25 s, and at T = 1.5 s the numerical heave motions of the moored circular and square cylinders are underestimated in comparison with the laboratory measurements. Furthermore, the numerical pitch motions of the circular cylinder is smaller than its measured motions in laboratory experiments at both incoming wave periods. However, both numerical and measured motions of the square cylinder are in good agreement at incoming wave periods T = 1.25 s and 1.5 s. Finally, it can be seen that by adding the mooring lines, the motions of both cylinders become smaller at T = 1.5 s, as expected.

Comparisons shown in Figs. 3 (a) and (b) represent a good agreement between the motions of the floating cylinders to combined wave and current loads, measured by laboratory experiments and computed by the boundary element method using the Green function for small forward speeds. Moreover, it can be seen that the effect of mooring lines on the motions of the cylinders are insignificant at the considered incoming wave periods and current speed.

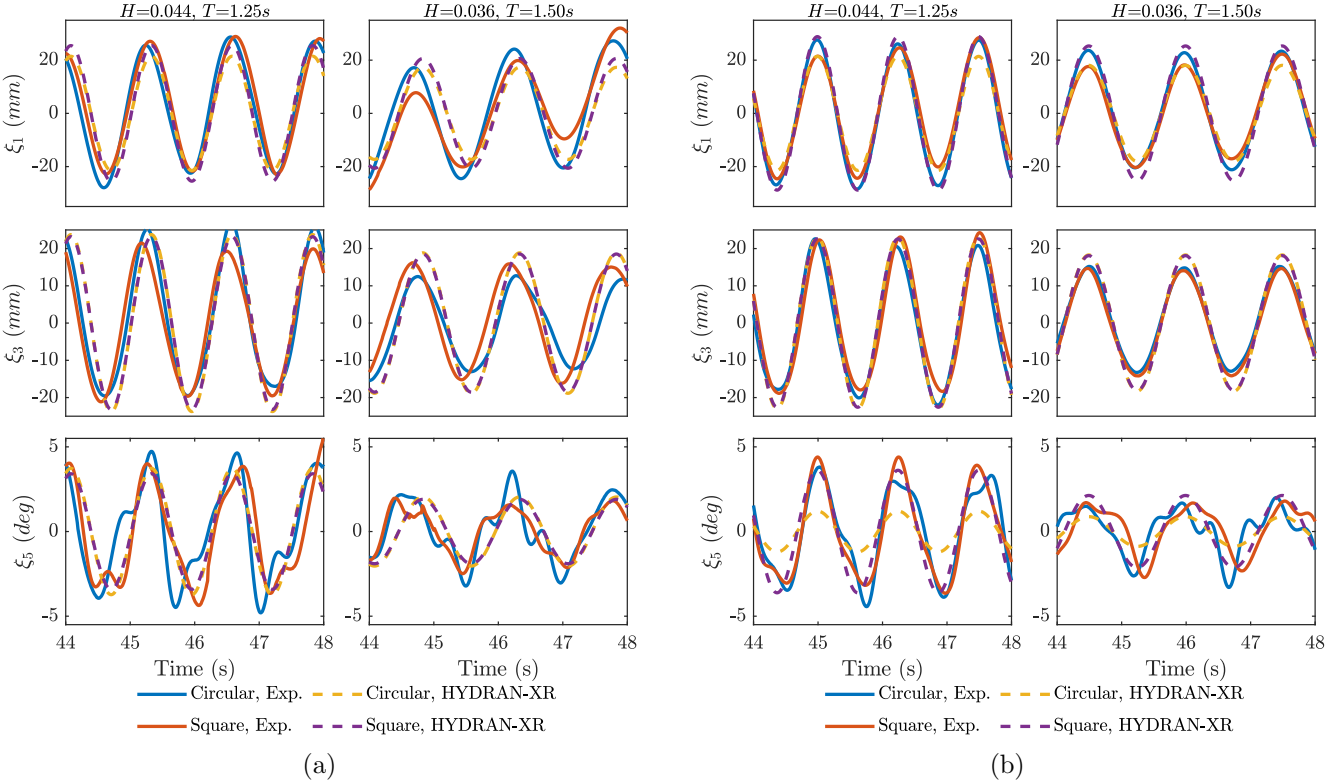

Figure 3: Comparison of the surge, heave and pitch time series of the (a) freely floating and (b) moored circular and square cylinders for two wave periods and wave heights.

References

Chen, X. B. & Malenica, Š. (1998), 'Interaction effects of local steady flow on wave diffraction-radiation at low forward speed', *International Journal of Offshore and Polar Engineering* **8**(2), 101–109.

Noblesse, F., Taylor, D. & Chen, X. B. (1995), 'Decomposition of free-surface effects into wave and near-field components', *Ship Technology Research* **42**(4), 167–185.

NumSoft Technologies (2020), Hydran-xr, hydrodynamic response analysis with integrated structural finite element analysis, version 20.1, Technical report, Numsoft Technologies.

Taylor, R. E. (1990), 'The hydrodynamic force on an oscillating ship with low forward speed', *Journal of Fluid Mechanics* **211**(333), 333–353.

Zhao, R. & Faltinsen, O. (1988), Wave-current interaction effects on large-volume structures, *in* 'Conference on Behaviour of Offshore Structures, June, Trondheim, Norway', number 1, June, Trondheim, Norway, pp. 187–190.